

Bandpass Filters with Localized Temperature Compensation in LTCC

Steve Dai and Lung-Hwa Hsieh

Sandia National Laboratories, Albuquerque, New Mexico, USA

sxdai@sandia.gov and lhsieh@sandia.gov

Low temperature cofired ceramic (LTCC) is a multilayer 3D packaging, interconnection, and passive integration technology. For LTCC modules with embedded resonator functions targeting radio frequency applications, the temperature coefficient of resonant frequency (τ_f) is a critical parameter. The base dielectrics of commercial LTCC systems have a τ_f in the range $-50 \sim -80 \text{ ppm}^\circ\text{C}$. This study explores a method to achieve zero or near zero τ_f embedded resonators by incorporating τ_f compensating dielectrics locally into a multilayer LTCC structure. A stripline bandpass filter (BPF) with near zero τ_f is demonstrated in a non-zero τ_f DuPont 951 GreenTape™ LTCC.

Key words: LTCC, τ_f , temperature compensation, filter

1. INTRODUCTION

Compact, low-cost, highly integrated passive and active component capabilities are sought after by wireless device manufacturers. The low temperature cofired ceramic (LTCC) is one of several attractive technologies that offers these capabilities. LTCC provides layout flexibility and three dimensional integration capabilities to produce embedded compact passive components, such as resistors, inductors, capacitors, filters, duplexers, and antennas [1-5]. External passive and active components can be surface mounted on LTCC boards to achieve low-cost, compact RF modules.

The mechanically-tuned temperature-compensated filters [6] and bulk-acoustic-wave (BAW) filters [7] demonstrated excellent temperature compensation. However, compared to LTCC filters, the mechanically-tuned filter was a larger size, and was difficult to integrate with other electronic components on printed-circuit-board. The BAW filters as individual components occupied more space and cost more than the embedded LTCC filters.

There were other approaches to obtain temperature stable bandpass filters [8-13]. One common method of realizing a near zero τ_f was to mix different dielectric ceramics that had opposite τ_f . This method has been applied to resonator and filter applications [8-9], as well as to those using LTCC base dielectrics [10-11]. The other method was to fabricate hybrid-layered structure where layers with opposite τ_f were formed into a monolithic stack by either sequential sintering [12] or bonding processes to obtain temperature compensation [13].

In this paper, strontium titanate SrTiO_3 (STO) based compensation dielectrics cofireable with DuPont 951 LTCC are characterized. A four-pole bandpass filter (BPF) incorporating the compensation dielectric is characterized over -20°C to 80°C to demonstrate the temperature stability.

2. TEMPERATURE COMPENSATION MATERIALS

The DuPont 951 GreenTape™ LTCC has a standard tape thickness of 0.254 mm before firing. The sintered LTCC dielectric has a dielectric constant of 7.88 and loss tangent of 0.006 at 3 GHz. The formulation and sintered density of STO compensation materials are listed in Table

I, where the V-glass enables cofiring of the compensation dielectric to DuPont 951 LTCC, the Al_2O_3 ceramic serves as filler material and STO is used to adjust τ_f . The weight fraction of the V-glass was fixed at 55wt%. The base formulation, designed as STO0, is 55wt% V-glass and 45wt% Al_2O_3 ceramic powders. Part of Al_2O_3 was replaced by STO to form a series of composition materials up to STO30. The mixture of V-glass, Al_2O_3 and SrTiO_3 was co-milled to a median particle size from 2.0 to 2.2 μm using Al_2O_3 media. Pellets of the compositions were pressed and sintered in air at 850°C for 30 minutes. Gold was sputtered on to both sides of the pellets for dielectric property measurement. The temperature dependent capacitance of the sintered pellets was measured using a HP4194A impedance analyzer at 1 MHz inside a temperature chamber.

Table I, Formulations and sintered density of STO compensation materials

Composition	V-glass (wt%)	Al_2O_3 (wt%)	SrTiO_3 (wt%)	Density (g/cc)
STO 0	55	45	0	3.19
STO10	55	35	10	3.21
STO20	55	25	20	3.30
STO25	55	20	25	3.31
STO30	55	15	30	3.35

τ_f is a device parameter that can be expressed using basic material properties:

$$\tau_f = -\frac{1}{2} \tau_\epsilon - \alpha \quad (1)$$

where τ_ϵ is the temperature coefficient of dielectric constant and α is the coefficient of thermal expansion (CTE). For LTCC dielectrics, α is typically between $4 \sim 10 \text{ ppm}^\circ\text{C}$, so τ_ϵ dominates τ_f . CTE of Dupont 951 LTCC dielectric is $5.8 \text{ ppm}^\circ\text{C}$. The τ_f of STO compositions can be obtained by measuring the capacitance of pellets over temperature and the τ_ϵ is calculated from the temperature dependence.

Table II shows the measured dielectric constant of DuPont 951, STO0, STO10, STO20, STO25 and STO30 over -20°C to 80°C . The dielectric constant normalized to that at 20°C of each composition was plotted in Fig. 1. As seen in Fig. 1, the STO0 has the same slope as that of DuPont 951 so this composition cannot be used to

compensate the temperature drift of the DuPont 951. In contrast, the STO30 has the greatest slope among the STO compositions that is opposite to that of 951 LTCC, thus it was selected to build temperature compensated bandpass filters. The best temperature compensation was achieved when the STO compensation materials were placed directly next to the strip line and the DuPont 951 was placed at outer layer close to ground [10].

TABLE II. Dielectric constants of DuPont 951, STO0, STO10, STO20, STO25, and STO30 over temperature.

Temperature (°C)	DuPont 951	STO 0	STO10	STO20	STO25	STO30
-20	7.84	7.74	9.57	12.4	14.12	16.17
0	7.86	7.76	9.57	12.33	13.99	15.98
20	7.88	7.79	9.57	12.27	13.88	15.82
50	7.91	7.83	9.57	12.2	13.75	15.64
80	7.94	7.89	9.59	12.15	13.66	15.45

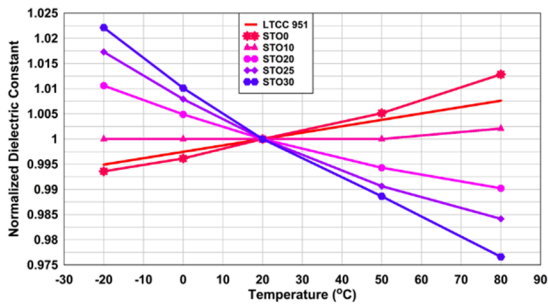


Fig.1, The diagram of the dielectric constants of DuPont 951 and STO dielectrics over temperature

3. TEMPERATURE COMPENSATED BPF

3.1 Filter design

Fig. 2 shows the layout of a wide stopband bandpass filter. The filter was designed at center frequency of 3.5 GHz with 3dB bandwidth of 500 MHz. The design procedure of finding the physical tapping at input and output locations as well as gap sizes between resonators can be found in reference [14].

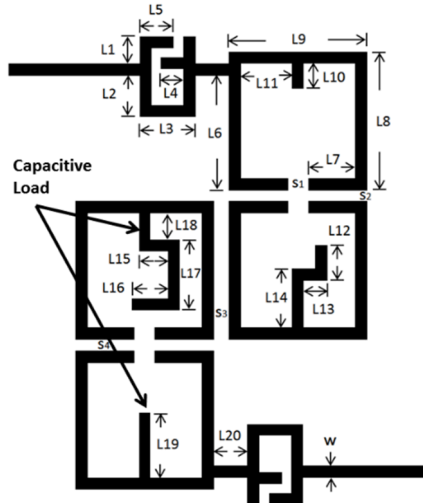


Fig. 2, Configuration of the bandpass filter.

The filter consists of capacitor-loaded open-loop ring resonators and lowpass filters. The effect of the capacitive loads at ring resonators is to push its harmonics to higher frequency range to obtain a wide stopband [15]. The

lowpass filters, at the input and output of the filter, are used to filter out harmonics of the capacitive load ring resonators, and also to obtain the wide-stopband effects [16].

The dimensions of the filter are: $w = 0.36$ mm, $L1 = 0.82$ mm, $L2 = 1.25$ mm, $L3 = 1.68$ mm, $L4 = 0.7$ mm, $L5 = 1.02$ mm, $L6 = 3.44$ mm, $L7 = 1.42$ mm, $L8 = 4.16$ mm, $L9 = 4.16$ mm, $L10 = 0.75$ mm, $L11 = 1.54$ mm, $L12 = 1.08$ mm, $L13 = 0.7$ mm, $L14 = 1.78$ mm, $L15 = 0.88$ mm, $L16 = 1.07$ mm, $L17 = 2.13$ mm, $L18 = 0.78$ mm, $L19 = 1.95$ mm, $L20 = 0.99$ mm, $s1 = 0.6$ mm, $s2 = 0.334$ mm, $s3 = 0.44$ mm, and $s4 = 0.328$ mm. The final fabricated bandpass filter is shown in Fig. 7. The size of the filter is 22.7 mm x 23.7 mm.

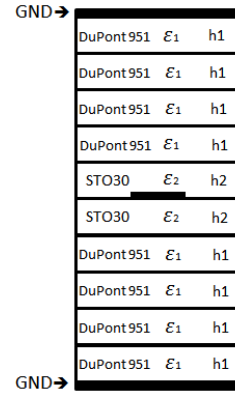


Fig. 3, Cross-section of the best temperature compensated configuration of DuPont 951 and STO30

The filter uses a 10-layer structure, shown as a cross sectional view in Fig. 3, with the thickness of STO30 optimized and set at $h2 = 40$ μm [17]. There are 4 LTCC layers on each side of the center strip line. The fired thickness of each layer is $h1 = 0.216$ mm. The final fabricated bandpass filter is shown in Fig. 4, as a 3-D see-through view, at a size 22.7 mm x 23.7 mm.

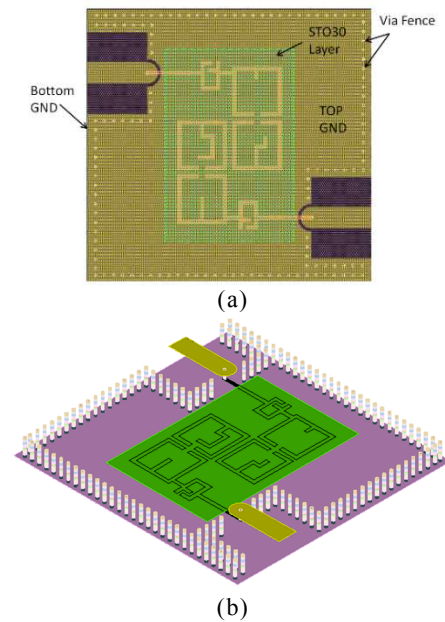


Fig. 4, (a) 2-D final fabricated bandpass filter, and (b) 3-D configuration without top ground plate.

3.2 Filter characterization

The measured frequency response of the filter is shown in Fig. 5(a). The filter was tested from -20°C to 80°C . The γ_f of the filter is $0.7 \text{ ppm}/^{\circ}\text{C}$. The insertion loss of the filter is 2.45 dB at 20°C . The insertion loss variance over the temperature is 0.28 dB . In Fig. 5(b), the maximum-difference group delay of the filter is 37 pS .

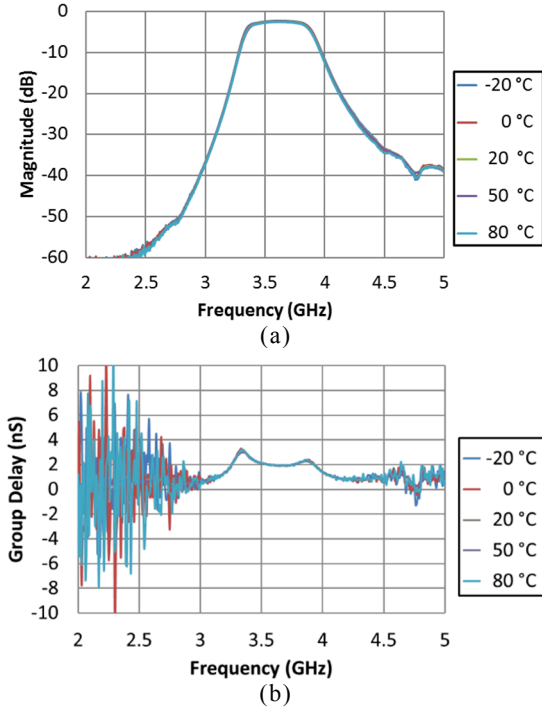


Fig. 5, (a) Measured S21 and (b) measured group delay of the filter over temperature.

The temperature coefficient of resonant frequency γ_f is calculated as:

$$\tau_f = \frac{1}{f_{ro}} \left(\frac{\Delta f_r}{\Delta T} \right) \quad (2)$$

where f_{ro} is the center frequency at 20°C , Δf_r is the change of the center frequency over -20 to 80°C , and ΔT is equal to 100°C . The center frequency is calculated by

$$f_{center} = \frac{f_{L_3dB} + f_{H_3dB}}{2} \quad (3)$$

where f_{L_3dB} is the 3dB frequency at low side of the passband and f_{H_3dB} is the 3 dB frequency at high side of the passband.

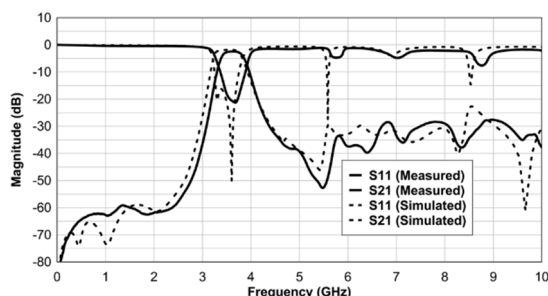


Fig. 6, Measured and simulated results of the filter.

Fig. 6 shows the measured and simulated wide-rage frequency response of the filter. The measured insertion loss of the filter is better than 2.45 dB , the stopband greater than 27.6 dB from 4.3 GHz to 10 GHz , and the 3 dB bandwidth is 0.5 GHz . The simulation is performed by using Agilent ADS EM simulator.

4. CONCLUSIONS

A temperature-compensated bandpass filter using modified SrTiO₃ materials cofirable with DuPont 951 LTCC is demonstrated. The filter has a temperature coefficient of resonant frequency $\gamma_f = 0.7 \text{ ppm}/^{\circ}\text{C}$. The insertion loss at 20°C is greater than 2.45 dB . The variance of insertion loss of the filter over the wide range temperature is 0.28 dB . The wide stopband is better than 27.6 dB from 4.3 to 10 GHz .

ACKNOWLEDGEMENT

Sandia National Laboratories is a multimission laboratory managed and operated by National Technology and Engineering Solutions of Sandia LLC, a wholly owned subsidiary of Honeywell International Inc. for the U.S. Department of Energy's National Nuclear Security Administration under contract DE-NA0003525.

REFERENCES

- [1] G. Brzezina and L. Roy, IEEE Trans. Compon. Packag. Manuf. Technol., **4**(1), 26–36 (2014).
- [2] H. C. Lu, T. W. Chao, Y. -L. Chang, T. -B. Chan and Y. T. Chou, IEEE Trans. Compon. Packag. Manuf. Technol., **1**(10), 1608–1615 (2011).
- [3] R. Amaya, A. Momciu, and I. HAroun, IEEE Trans. Compon. Packag. Manuf. Technol., **3**(3), 411–416 (2013).
- [4] H. C. Chen, C. H. Tsai, and T. L. Wu, IEEE Trans. Compon. Packag. Manuf. Technol., **2**(6), 1030–1038 (2012).
- [5] C. W. Tang and H. C. Hsu, IEEE Trans. Microwave Theory Tech, **5**(8), 624–634 (2010).
- [6] J. Ju, IEEE Trans. Microwave Theory Tech, vol. 52, no. 1, 139–143, (2004).
- [7] N. Hu, C. Zhou, W. Pang and H. Zhang, Proceedings of Asia-Pacific Microwave Conf., 1102-1105 (2011).
- [8] W. Wersing, Solids State and Mat Sci, **1**(5) 715–731 (1996).
- [9] I. M. Reaney, and D. Iddles, J. Am. Ceram Soc, **89**, 2063-2072 (2006).
- [10] S. Dai, R. Huang and D. Wilcox, J. Am. Ceram. Soc, **85**, 828-832 (2002).
- [11] Y. Choi, J. Park, J. G. Park, Materials Letters, **58**, 3102– 3106 (2004).
- [12] J. Breeze, S. J. Penn, M. Poole and N. Alford, **36**(10), 883-885 (2000).
- [13] L. Li and X. M. Chen, J. Am. Ceram. Soc., **89**, 544–549 (2006).
- [14] J. S. Hong and M. J. Lancaster, Microstrip Filters for RF/Microwave Applications. New York, NY, USA: Wiley, 2001
- [15] S. R. Wu, K. W. Hsu, and W. H. Tu, **6**(13) 1422-1428 (2012).
- [16] L. H. Hsieh and K. Chang, IEEE Trans. Microw. Theory Tech., **54**(10), 193–199 (2003).
- [17] L. H. Hsieh and S. Dai, IEEE Trans on Compon, Packag. and Manuf. Tech., **4**(9) 1427-31 (2014).